Brain, Behavior, and Immunity 81 (2019) 617–629

Contents lists available at ScienceDirect

Brain, Behavior, and Immunity

journal homepage: www.elsevier.com/locate/ybrbi

Lactobacillus rescues postnatal neurobehavioral and microglial dysfunction in a model of maternal microbiome dysbiosis

Yeonwoo Lebovitz[a], Elizabeth A. Kowalski[b], Xia Wang[b], Colin Kelly[c], Madison Lee[c], Valerie McDonald[d], Rachael Ward[c], Miranda Creasey[e], William Mills[a], Erwin Kristobal Gudenschwager Basso[b], Amanda Hazy[b], Terry Hrubec[b,d], Michelle H. Theus[a,b,c,f,*]

[a] Graduate Program in Translational Biology, Medicine, and Health, Virginia Tech, Blacksburg, VA 24061, USA
[b] Department of Biomedical Sciences and Pathobiology, VA-MD College of Veterinary Medicine, Blacksburg, VA 24061, USA
[c] School of Neuroscience, Virginia Tech, Blacksburg, VA 24061, USA
[d] Department of Biomedical Sciences, Edward Via College of Osteopathic Medicine, Blacksburg, VA 24060, USA
[e] Virginia Tech Carilion School of Medicine, Roanoke, VA 24016, USA
[f] Center for Regenerative Medicine, VA-MD College of Veterinary Medicine, Blacksburg, VA, 24061, USA

ARTICLE INFO

Keywords:
Cx3cr1
Gut bacteria
Microbiota
Social behavior
Trp53
Senescence
Neurodevelopment
Autism spectrum disorders

ABSTRACT

Increasing reports of pregnancy events leading to maternal microbiome dysbiosis (MMD) show strong correlates with atypical neurodevelopmental outcomes. However, the mechanism(s) driving microbiome-mediated behavioral dysfunction in offspring remain understudied. Here, we demonstrate the presence of a novel gut commensal bacterium strain, *Lactobacillus murinus* HU-1, was sufficient to rescue behavioral deficits and brain region-specific microglial activation observed in MMD-reared murine offspring. We further identified a postnatal window of susceptibility that could prevent social impairments with timed maternal administration of the symbiotic bacterium. Moreover, MMD increased expression of microglial senescence genes, *Trp53* and *Il1β*, and Cx3cr1 protein in the prefrontal cortex, which correlated with dysfunctional modeling of synapses and accompanied dysbiosis-induced microglial activation. MMD male offspring harboring *Lactobacillus murinus* HU-1 or lacking *Cx3cr1* showed amelioration of these effects. The current study describes a new avenue of influence by which maternally transferred *Lactobacillus* drives proper development of social behavior in the offspring through microglia-specific regulation of Cx3cr1 signaling.

1. Introduction

An emerging evidence base of large-scale, retrospective epidemiological studies on pregnancy risk factors for neurodevelopmental disorders have converged on acute fever, severe infections, and broad spectrum antibiotic use as significant correlates of mental disorders, such as autism and schizophrenia (Al-Haddad et al., 2019; Atladottir et al., 2012; Jiang et al., 2016; Lee et al., 2015; Lydholm et al., 2019). Acute fever and severe infections during pregnancy are directly attributed to maternal immune activation and subsequent disruptions to fetal development, including that of the central nervous system (Choi et al., 2016; Mortensen et al., 2007; Smith et al., 2007). Meanwhile, antibiotics represent the most prescribed medication during pregnancy and early postpartum periods (Andrade et al., 2004). These factors are hypothesized to disrupt maternal microbiota and influence the critical microbial inoculum that is transferred from mother to child. However, the exact nature of the relationship between bacteria-related microbiome dysbiosis and atypical neurodevelopment remains unclear.

Under typical conditions, symbiotic bacteria in the gut, vagina, skin, and breast are uniquely consolidated around specific groups (e.g., *Lactobacillus*) and these specialized microbial environments are thought to be necessary for maintaining immune balance and for priming the naïve immune system (Backhed et al., 2015; Nuriel-Ohayon et al., 2016; Sharon et al., 2016; Vuong et al., 2017). Accordingly, germ-free conditions result in the aberrant development of resident microglia in the brain, which can be rescued by restoring a complex microbiota (Erny et al., 2017; Hammond et al., 2018). These effects have been postulated to have a major impact on microglial functions, including maintenance of synapses and control of neuroinflammation. Moreover, these findings suggest the gut-brain axis is central in supporting normal neuron-

* Corresponding author at: Center for Regenerative Medicine, Department of Biomedical Sciences and Pathobiology, College of Veterinary Medicine, Virginia Tech, 970 Washington Street SW (MC0910), Blacksburg, VA 24061, USA.
E-mail address: mtheus@vt.edu (M.H. Theus).

https://doi.org/10.1016/j.bbi.2019.07.025
Received 29 May 2019; Received in revised form 10 July 2019; Accepted 23 July 2019
Available online 24 July 2019

microglia communication. Recent studies also demonstrate that *Lactobacillus* species can correct social impairments in several mouse models of autism due to afferent vagal nerve regulation of brain regions involved in social reward (Sgritta et al., 2019). The exact mechanism(s) of action underlying the role of gut microbiota on social development remains unclear.

Animal models of gut dysbiosis, whether due to reduced bacterial diversity or complete germ-free status, indicate that the microglia in the adult offspring show aberrations with respect to morphology, functionality, and expression of inflammatory genes (Erny et al., 2015; Matcovitch-Natan et al., 2016; Thion et al., 2018). Adult offspring reared under altered gut microbial conditions exhibit behavioral anomalies likened to autism-like symptoms, such as a lack of social preference (Leclercq et al., 2017; Tochitani et al., 2016). Importantly, microglial and behavioral anomalies could be rescued in adult mice with microbiome dysbiosis following re-introduction of healthy gut microbiota and/or mono-colonization with a symbiotic bacterium, such as *Lactobacillus* (Diaz Heijtz et al., 2011; Erny et al., 2015; Jang et al., 2018). While these studies highlight microbiota effects in adult brain and behavior, little is known about the cellular and molecular mechanism(s) regulating these changes during perinatal development and whether they can be similarly rescued through probiotic interventions.

A cross-disciplinary examination of studies from gut immunology and neurodevelopment suggests a potential avenue of microbiota-gut-brain signaling via the chemokine receptor, Cx3cr1, which is expressed on macrophages, natural killer cells, and certain subsets of T cells and dendritic cells (Panek et al., 2015). In the brain, Cx3cr1 is primarily expressed on microglia where it serves as the specific receptor for neuronally expressed Cx3cl1 (fractalkine), a transmembrane glycoprotein that can be released by neurons after proteolytic cleavage under cytotoxic or other stimuli (Paolicelli et al., 2014). A major form of cross-talk between microglia and neurons in the brain is the Cx3cr1-Cx3cl1 pathway, which is instrumental in regulating synaptic pruning and limiting microglial activation. Interestingly, neuronal fractalkine expression is regionally restricted to areas of the brain known to regulate social behavior, such as the cortex, hippocampus, and amygdala. Due to the emerging role that Cx3cr1 plays in both the gut and brain, it represents an important pathway to evaluate microglia-neuron interactions in response to dysbiosis in the context of neurodevelopment (Dorfman et al., 2017; Verheijden et al., 2015).

In the present study, we developed an antibiotics-based bacterial depletion model of maternal microbiota dysbiosis (MMD) with which to study neurobehavioral development and microglial responses in the offspring. Notably, we identified a novel postnatal window of susceptibility where social deficits and microglial activation observed in MMD offspring can be prevented with timed administration of a symbiotic, antibiotic-resistant gut bacterium, *Lactobacillus murinus* HU-1 (MMD^{Lacto}). We further show that MMD-induced microglial activation is accompanied by increased expression of senescence genes, *Trp53* and *Il1β*, and microglia-specific Cx3cr1 protein in the prefrontal cortex, the loss of which ($Cx3cr1^{GFP/GFP}$) also rescued MMD-induced social and microglial dysfunction. Our novel findings demonstrate that maternal gut dysbiosis mediates dysregulation of key cellular and molecular pathways that regulate social behavior in murine offspring.

2. Results

2.1. Model of maternal microbiome dysbiosis (MMD) and treatment with L. murinus HU-1

To determine whether disrupting the maternal gut microbiome influences neurobehavioral outcomes in the offspring, we utilized an antibiotics-based model of maternal microbiome dysbiosis (MMD) by administering an antibiotic cocktail via drinking water to both female and male mice one week prior to breeding and producing offspring for behavioral and histological assessments (Fig. 1A). MMD mice were maintained on antibiotic drinking water throughout gestation and parturition until time of offspring weaning at postnatal day 21 (P21). Due to previous evidence of neuroprotective effects of probiotics, such as *Lactobacillus rhamnosus* JB-1 (Leclercq et al., 2017) and *L. reuteri* (Sgritta et al., 2019) in adult mice, we added a second group of MMD mice that were pretreated with an oral dose of our lab-generated strain of commensal gut bacterium, *L. murinus* HU-1. *L. murinus* HU-1 is an antibiotic-resistant strain of *L. murinus*, a common gut bacterium found in many mammal species with potential probiotic applications (Gardiner et al., 2004; Greetham et al., 2002; Vasconcelos et al., 2003). It is a key component of the Altered Schaedler Flora that is genetically similar to other food fermenter bacteria, such as *L. animalis* (Fig. 1B) (Sarma-Rupavtarm et al., 2004; Schaedler et al., 1965; Wymore Brand et al., 2015). To examine the effects of *L. murinus* HU-1 on the neurodevelopmental outcomes following MMD exposure, mice were treated for three days with *L. murinus* HU-1 via oral gavage prior to the onset of MMD (MMD^{Lacto}) while the control untreated groups were maintained under conventional specific pathogen-free housing (CONV) (Fig. 1A).

MMD status was evident in the enlarged cecum size of MMD dams compared to CONV, which indicated the inability to properly break down food fibers due to gut dysbiosis. MMD^{Lacto} dams also exhibited enlarged cecum sizes which demonstrated the presence of *L. murinus* HU-1 was insufficient to fully restore the gut microbiota to a conventional state (Fig. 1C). MMD and MMD^{Lacto} status was regularly tested in breeding mice for the presence of 16s rRNA and *L. murinus*, respectively (Supplemental Fig. 1A). Next, 16s rRNA sequencing of maternal fecal bacteria was performed to assess the impact of MMD on gut microbiota composition. At the phylum level, CONV and MMD^{Lacto} dams shared similar gut microbial composition primarily consisting of *Firmicutes* and *Bacteroidetes* bacteria, whereas MMD dams were characterized predominantly by *Proteobacteria* (Fig. 1D). At the genus level, however, MMD^{Lacto} dams exhibited a distinct microbial profile from CONV dams with comparatively low diversity of bacteria genera and primarily consisted of *Lactobacillus* and *Parabacteroides*, which was replicated in microbial profiles of male offspring at P21 (Supplemental Fig. 1B). Although RT-PCR of MMD dams' fecal bacteria showed near complete depletion of gut bacteria (Supplemental Fig. 1A), deep sequencing identified numerous genera of bacteria in MMD dams' feces that can be characterized as environmental bacteria with pathogenic potential (e.g., *Xanthomonadaceae* and *Acinetobacter*) (LaSala et al., 2007; Wong et al., 2017). These treatment-specific differences in maternal microbiota were consistent in dams and offspring across different mouse strains (outbred CD-1 versus inbred $Cx3cr1^{GFP/GFP}$) (Fig. 1D and Supplemental Fig. 1B).

Recent studies of the gut-brain axis revealed that gut bacteria-derived metabolites likely serve neuroactive roles and are capable of passing the placental and blood-brain barriers to modulate neural function and behavior (Braniste et al., 2014; Erny et al., 2015; Sampson and Mazmanian, 2015; Vuong et al., 2017). To test whether MMD status during pregnancy may influence expression of gut bacteria-related metabolites, we performed chemical analysis of CD-1 maternal feces via gas chromatography. We found a significant reduction in three prominent gut bacteria-derived metabolites (acetic acid, propionic acid, and butyric acid) in both MMD (7.818 ± 1.471 mmol/L, 0.0 ± 0.0 mmol/L, 0.0 ± 0.0 mmol/L, respectively) and MMD^{Lacto} (9.761 ± 1.058 mmol/L, 0.0 ± 0.0 mmol/L, 0.0 ± 0.0 mmol/L, respectively) compared to CONV (25.63 ± 4.315 mmol/L, 4.558 ± 1.291 mmol/L, 4.592 ± 1.580 mmol/L, respectively) (Fig. 1E–G). Interestingly, MMD dams exhibited a significant increase in isovaleric acid (0.02 ± 0.01 mmol/L) compared to MMD^{Lacto} (0.0 ± 0.0 mmol/L) and CONV (0.0 ± 0.0 mmol/L) (Fig. 1H). Whereas both MMD and MMD^{Lacto} dams displayed increased levels of isocaproic acid (0.391 ± 0.125 mmol/L and 0.598 ± 0.219 mmol/L) and heptanoic acid (20.69 ± 3.602 mmol/L and 17.78 ± 1.09 mmol/L) compared to CONV dams (0.0 ± 0.0 mmol/L and 6.888 ± 1.432 mmol/L, respectively) (Fig. 1I and J). These findings

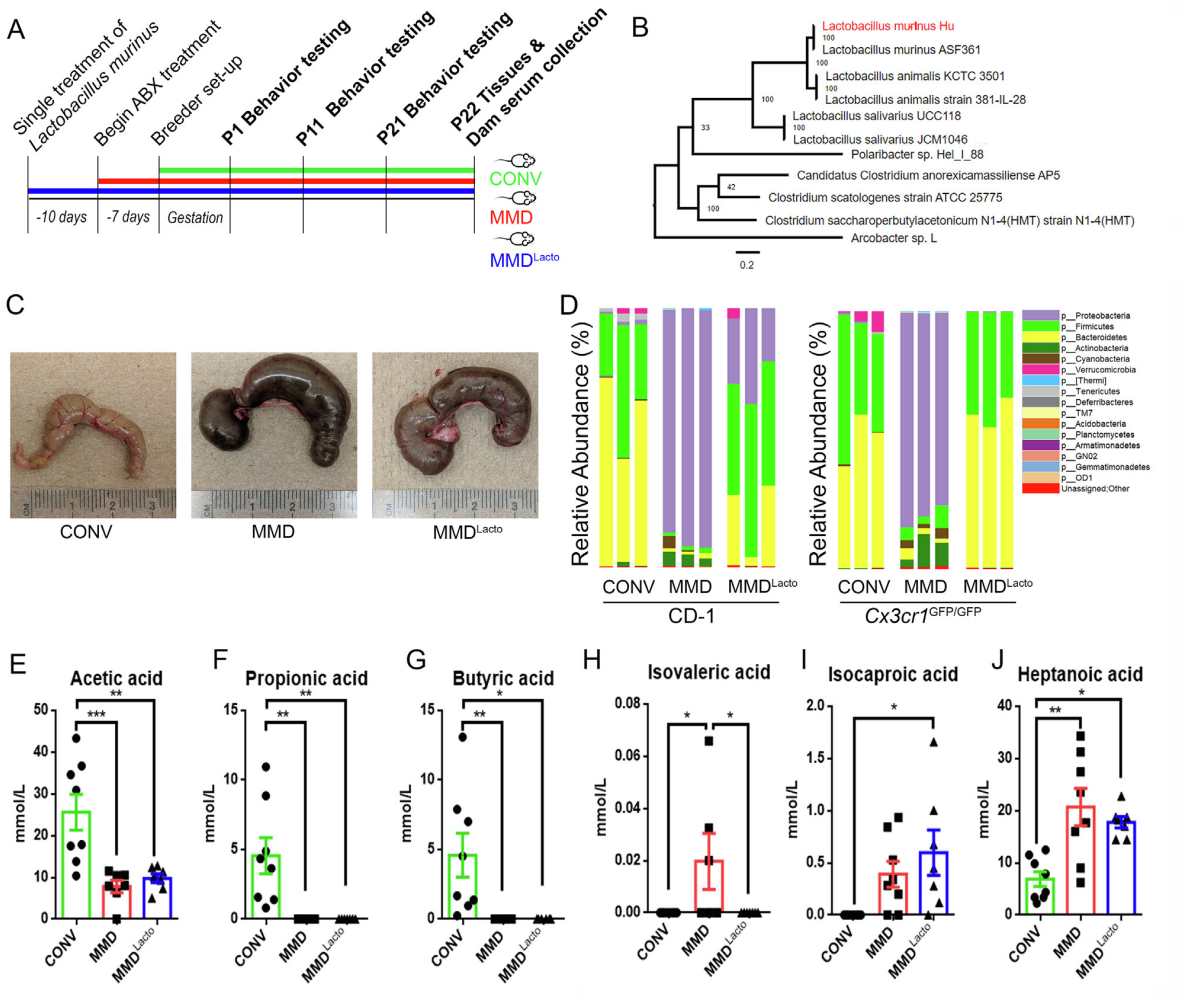

Fig. 1. Maternal microbiome dysbiosis (MMD) results in distinct maternal gut microbiome profiles. (A) Study design schematic for treatment times, breeding, and offspring assessment for conventionally-housed dams (CONV), antibiotics-treated dams (MMD), and MMD dams pre-treated with *Lactobacillus murinus* HU-1 (MMD^{Lacto}) in two strains, CD-1 and *Cx3cr1*-GFP breeders. (B) Phylogenetic tree of lab-generated *L. murinus* HU-1 with nearest-neighbor analysis indicate closest similarity to food fermenting species, *L. animalis*. (C) MMD dams at time of offspring weaning exhibit enlarged cecum size compared to CONV and MMD^{Lacto} dams. (D) Relative abundance of maternal fecal bacteria shows similarity between CONV and MMD^{Lacto}-treated dams at the phylum level regardless of mouse strain with predominantly *Firmicutes* and *Bacteroidetes* bacteria, whereas MMD dams show *Proteobacteria* abundance (n = 3 dams per group). (E-J) Maternal fecal levels of short-chain fatty acids, acetic acid, propionic acid, butyric acid, isovaleric acid, isocaproic acid, and heptanoic acid, respectively. (n = 7–8 dams per group). *P < 0.05, **P < 0.05, and ***P < 0.001.

demonstrate MMD induced significant remodeling of the maternal gut microbiota and resulted in altered production of key gut bacteria-derived metabolites. The presence of *L. murinus* HU-1 during MMD treatment partially prevented maternal gut dysbiosis, but could not recover altered production of most bacterial metabolites.

2.2. *L. murinus* HU-1 attenuates MMD-induced social deficits in offspring

To evaluate whether MMD status influences postnatal (P) offspring behavior, a battery of developmental tests on CD-1 neonatal pups were performed at P1, P11, and at weaning on P21. These dates were selected to provide longitudinal measurements across three distinct time points in murine postnatal development (Chen et al., 2017; Theiler, 1972). Both male and female pups from the first litter of each experimental dam were tested for physical, reflexive, gross motor, and social milestones. Four to six individual dams were used per experimental group with an average of 9 pups per litter, totaling approximately 45 pups tested per group. At P1, neonatal pups weighed and performed similarly in cliff aversion and negative geotaxis tests regardless of the treatment group (Fig. 2A–C). However, offspring born to MMD dams showed reduced righting ability compared to CONV and MMD^{Lacto} offspring (Fig. 2D). While no significant weight differences or righting ability were found at P11 across treatment groups (Fig. 2E, H), MMD offspring showed deficits in cliff aversion and negative geotaxis tests compared to CONV and MMD^{Lacto} (Fig. 2F and G). These atypical findings were corrected by P21, as pups performed similarly in all three behavioral tests regardless of treatment (Fig. 2I–L). However, differences arose with respect to the three-chamber social test wherein MMD offspring exhibited a lack of social preference compared to CONV and MMD^{Lacto} offspring (Fig. 2M).

Given that the prenatal presence of *L. murinus* HU-1 (MMD^{Lacto}) can reverse the postnatal behavioral deficits observed in MMD offspring, we sought to identify whether this was temporally restricted. To ascertain this, MMD dams were re-conventionalized at parturition by placing

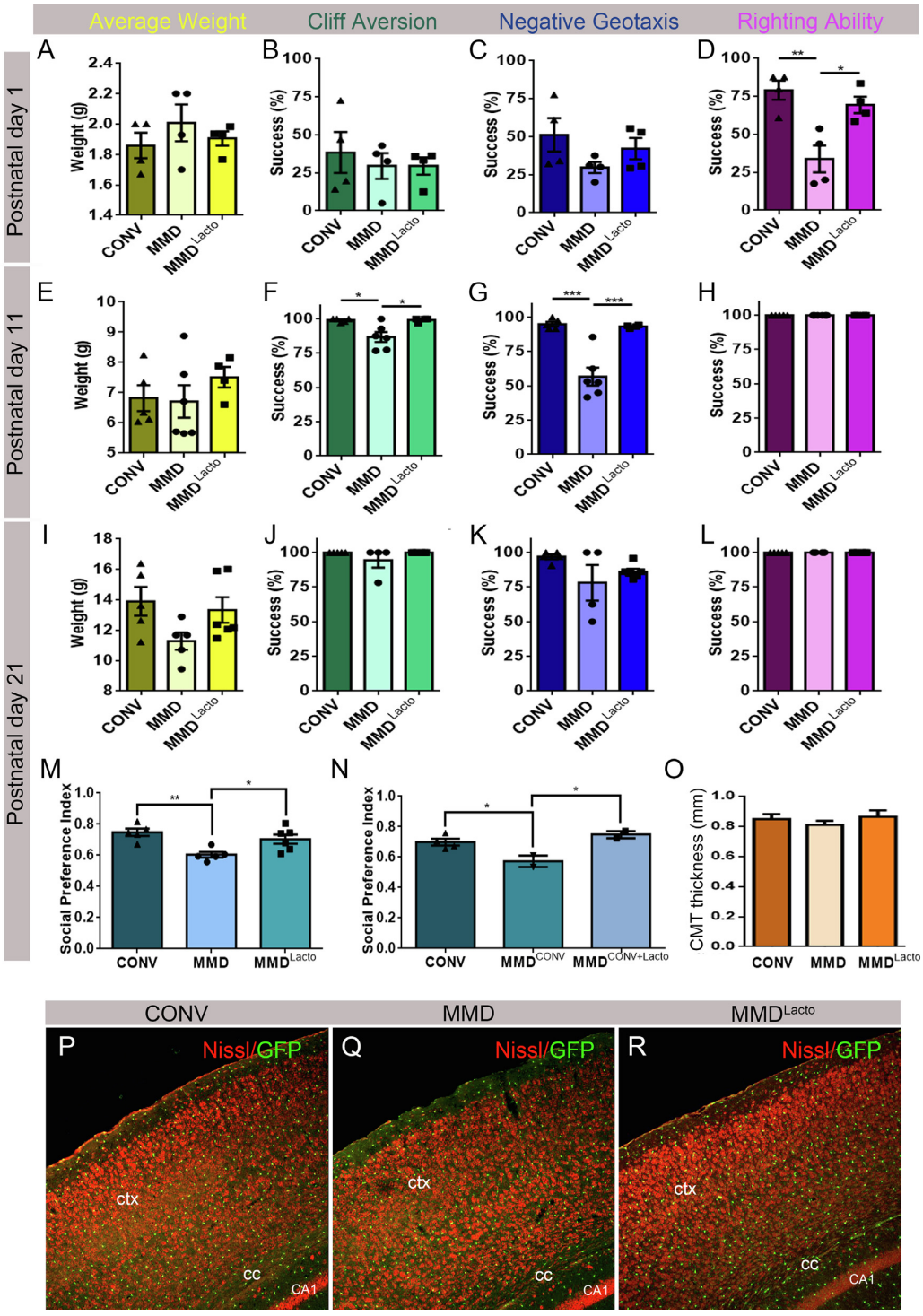

Fig. 2. MMD results in offspring with gross motor developmental delays and impaired social behavior that are attenuated in the presence of *L. murinus* HU-1. (A-D) At P1, MMD offspring show significant deficit in righting reflex test, whereas MMD^{Lacto} perform similarly to CONV. (E-H) At P11, MMD offspring exhibit new deficits in cliff aversion and negative geotaxis tests, whereas MMD^{Lacto} remain comparable to CONV. (I-L) At P21, previous gross motor deficits are recovered in MMD offspring. (M) MMD offspring exhibit lack of social preference in three-chamber test compared to CONV and MMD^{Lacto}. (N) Re-conventionalization of MMD dams (MMD^{CONV}) near parturition does not rescue social deficits. Re-conventionalization of MMD dams plus oral dosing with *L. murinus* HU-1 ($MMD^{CONV+Lacto}$) results in rescue of these behaviors. (O) No gross difference was observed in cortical mantle thickness between treatment groups. (P-R) Representative fluorescent confocal images of the parietal cortex stained with Nissl (red) and GFP for microglia. (n = 4–6 litters per group, average 38–49 pups per group). *P < 0.05, **P < 0.05, and ***P < 0.001.

them inside conventional housing (MMD^{CONV}) while a separate group of MMD dams were placed in conventional housing and provided a single oral dose of *L. murinus* HU-1 bacterium ($MMD^{CONV+Lacto}$) (Supplemental Fig. 2A). Gut microbiota and *L. murinus* HU-1 re-colonization were confirmed using RT-PCR (Supplemental Fig. 2B). Although MMD^{CONV} fecal DNA analysis showed recolonization with bacteria by 16s rRNA as early as 2 days following re-conventionalization, *L. murinus* could not be detected until 60 days later. In contrast, $MMD^{CONV+Lacto}$ fecal DNA analysis showed immediate recolonization with 16s rRNA and *L. murinus* at 3 days following re-conventionalization (Supplemental Fig. 2B). Offspring from recolonized MMD dams were then evaluated against the same battery of behavior tests as described above. Neither recolonization strategies fully corrected the atypical behaviors induced by MMD at P1 or P11 (Supplemental Fig. 2C–E). Although the MMD^{CONV} pups displayed the same social deficits as MMD pups at P21, the $MMD^{CONV+Lacto}$ pups showed amelioration of social dysfunction (Fig. 2N). Finally, we show no gross difference in cortical thickness between the treatment groups at P21 (Fig. 2O–R). These findings suggest postnatal gut-brain axis dysregulation is a major driver of the development of social impairments in mice and that postnatal microbiota recolonization required the presence of *L. murinus* HU-1 to restore typical social behavior.

2.3. L. murinus HU-1 rescues MMD-induced microglial morphological changes and Cx3cr1 alterations in the prefrontal cortex

Next, we asked whether the social deficits found in MMD offspring correlated with impaired microglia morphology and Cx3cr1 expression. To visualize the morphology of microglia in the brain, we stained serial coronal sections and performed confocal image analysis of the prefrontal cortex of male $Cx3cr1^{GFP/+}$ offspring at P21 from CONV, MMD, and MMD^{Lacto} breeders (Fig. 3A–C, respectively), which express green fluorescent protein in microglia of the brain. Compared to CONV and MMD^{Lacto}, MMD microglia exhibited highly dystrophic, fragmented processes and spheroid soma indicative of cytoplasmic deterioration and atrophy (Fig. 3B) (Streit et al., 2014). This dystrophic state did not correlate with greater overlap or co-labeling of GFP and neurite process marker neurofilament (Fig. 3B1–3) indicating these cells are not actively engulfing neuronal elements. Moreover, staining for Cx3cr1 revealed increased expression in the soma and processes of microglia of MMD offspring brains (Fig. 3E, I) compared to CONV (Fig. 3D, I) and MMD^{Lacto} (Fig. 3F, I). Together, these data show MMD treatment induced dystrophic morphology in MMD microglia, which may be the direct result of Cx3cr1 overexpression and impaired functional state.

2.4. MMD induces significant gene expression changes in cortical microglial

In an effort to elucidate how the presence of *L. murinus* HU-1 mitigated behavioral and microglial changes in MMD offspring, GFP^+ microglia were purified by FACS from the cortices of P22 $Cx3cr1^{GFP/+}$ heterozygous male offspring reared from MMD, MMD^{Lacto}, and CONV dams followed by RNAseq analysis. Comparative analysis found a small number of differentially-expressed genes from MMD and MMD^{Lacto} offspring with an even smaller set of heterogeneous genes shared between the two treatment groups (Fig. 4A and B) (Hulsen et al., 2008). Gene ontology enrichment analysis of MMD cortical microglia genes again showed a heterogeneous assortment of upregulated and downregulated genes with the largest grouping of genes related to metabolic processes (Fig. 4C and D) (Carmona-Saez et al., 2007; Nogales-Cadenas et al., 2009; Tabas-Madrid et al., 2012). Of these, MMD upregulated genes, such as *Acot1* in acyl-CoA degradation, represented opposing biological processes of downregulated genes, such as *Acsl6* in acyl-CoA synthesis. MMD^{Lacto} microglia also predominantly expressed genes related to metabolic processes, but frequently in the opposite manner of MMD. For example, while *Hdhd3*, *Rnf19a*, *Fn3k*, *Tst*, and *Car4* were downregulated in MMD microglia, the same genes were significantly upregulated in MMD^{Lacto} microglia (Supplemental Fig. 3) (Mi et al., 2019).

Prior studies using the maternal immune activation model suggested microglial inflammation as the key driver of dysfunction (Hammond et al., 2018; Lenz and Nelson, 2018). However, our model of MMD appeared to induce microglial effects beyond immune signaling, including expression of genes relevant to cell cycle, senescence, and cell aging. Closer examination of target genes by qPCR provided further validation and emphasized the increased differential expression of *Il1β* (Fig. 4E), *Ccr3* (Fig. 4F) and *Trp53* (Fig. 4G), while reduced expression was seen for *Hdac5* (Fig. 4H), *C1qc* (Fig. 4I) and *Cd68* (Fig. 4J) in MMD microglia compared to CONV and MMD^{Lacto}. These results support our RNAseq findings and suggest that MMD conditions may induce an immune-mediated senescent phenotype in microglia.

2.5. MMD-induced expression of CD68 is attenuated by L. murinus HU-1 and loss of Cx3cr1

We further examined the functional state of microglia following MMD in the presence and absence of *L. murinus* HU-1 treatment by staining for CD68, a lysosomal protein implicated in antigen processing by macrophages and a marker for microglial activation (Chistiakov et al., 2017; Korzhevskii and Kirik, 2016). Importantly, given the overexpression of Cx3cr1 found on MMD microglia, which is restored in MMD^{Lacto}, we sought to evaluate whether loss of Cx3cr1 may affect these changes. Therefore, we utilized $Cx3cr1^{GFP/GFP}$ knockout and $Cx3cr1^{GFP/+}$ heterozygous P22 male offspring reared from CONV, MMD, and MMD^{Lacto} breeders. Serial coronal sections were evaluated for $GFP^+/CD68^+$ immunoreactivity and quantified in the cortex and hippocampal regions due to their associations with complex behaviors that frequently underlie neurodevelopmental disorders (Edmonson et al., 2014; Gacias et al., 2016; Morgan et al., 2010). Non-biased stereology showed no quantifiable differences in the total number of GFP^+ microglia across treatments and genotypes. However, the number of $GFP^+/CD68^+$ cells was significantly increased in the parietal (Fig. 5A) and prefrontal cortex (Fig. 5C) of $Cx3cr1^{GFP/+}$ MMD compared to $Cx3cr1^{GFP/+}$ CONV mice at multiple bregma levels (Supplemental Fig. 4). Hippocampal regions largely did not exhibit differences across treatment groups, except at bregma −2.6 in which MMD mice showed increased $GFP^+/CD68^+$ cells compared to CONV (Fig. 5B and Supplemental Fig. 4). Importantly, this effect was abrogated in $Cx3cr1^{GFP/GFP}$ knockout mice and in mice treated with *L. murinus* HU-1. Similar findings were found when analyzing the proportion of GFP^+ cells that were $CD68^+$ versus $CD68^-$ (Fig. 5D–I). While similar assessment of the total numbers of prenatal GFP^+ and $CD68^+/GFP^+$ microglia at E17 did not show any significant changes following MMD (Supplemental Fig. 5A), both MMD and MMD^{Lacto} treated $Cx3cr1^{GFP/+}$ pups showed increased proportions of $CD68^+/GFP^+$ versus $CD68^-/GFP^+$ cells compared to CONV or $Cx3cr1^{GFP/GFP}$ knockout treated mice (Supplemental Fig. 5B), and suggest the rescue effects by *L. murinus* HU-1 are due to mechanism(s) present after the gut becomes colonized by bacteria following birth. Collectively, our data indicate MMD drives microglial activation in specific brain regions, which are highly regulated by Cx3cr1 signaling.

2.6. Cx3cr1 signaling mediates MMD-induced social deficits and PSD-95 cortical expression

Lastly, we evaluated whether the effects of Cx3cr1 loss-of-function on preventing MMD deficits in microglia correlated with changes in social behavior. We found $Cx3cr1^{GFP/+}$ MMD mice replicated the social deficits previously observed in CD-1 MMD offspring and also showed restored social preference in the presence of *L. murinus* HU-1. Both male and female offspring were tested from 4 to 5 individual dams per experimental group with an average of 7 pups per litter and approximately 29.5 pups per group. Interestingly, loss of *Cx3cr1* attenuated

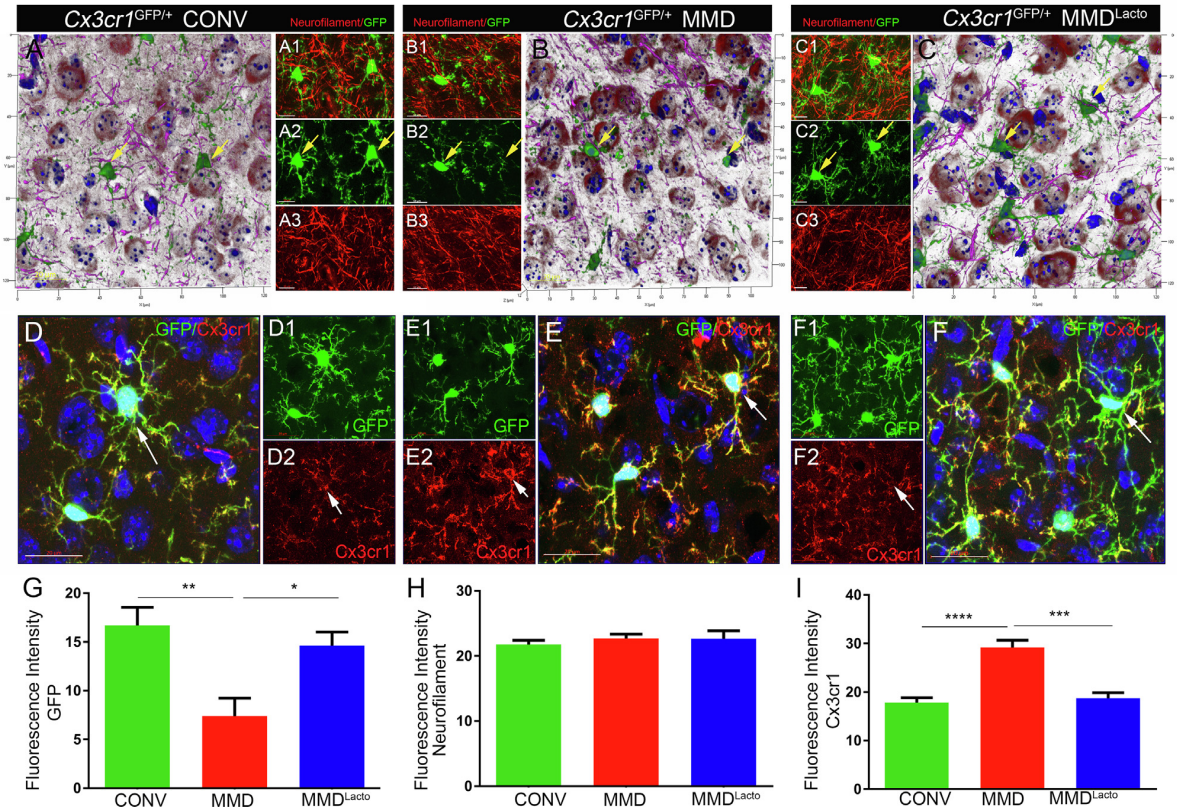

Fig. 3. MMD male offspring exhibit microglial dystrophy and increased Cx3cr1 expression in the prefrontal cortex. Representative confocal images analysis of GFP$^+$ microglia using *Cx3cr1*$^{GFP/+}$ male offspring under CONV, MMD, and MMD^{Lacto} conditions. (A-C) 3D rendering of z-stack images from serial sections tripled labeled with GFP, Nissl (red), and neurofilament (pink). Insets represent single channel images of GFP+ microglia and co-labeling for neurite processes showing microglia morphology. (D-F) Z-stack maximum projected confocal images showing Cx3cr1 (red) in each condition shows increased expression in microglial soma and processes under MMD, compared to CONV and MMD^{Lacto}. Scale = 10 μm in A1-A3, B1-B3 and C1-C3. Scale = 20 μm in D-F. (G-I) Quantification of fluorescence intensity of GFP (G), neurofilament (H), and Cx3cr1 expression (I). (n = 5 mice per group). *P < 0.05, **P < 0.05, ***P < 0.001, and ****P < 0.0001.

social deficits induced by MMD (Fig. 6A). Furthermore, sex-specific analysis of social preference behavior in *Cx3cr1*$^{GFP/+}$ mice indicated similar pattern between male and female offspring with no significant interaction between sex and treatment (Fig. 6B).

Given the role of Cx3cr1 in mediating MMD-induced microglial activation and behavioral changes, we quantified excitatory post-synaptic protein, PSD-95, in the cortices of *Cx3cr1*$^{GFP/+}$ and *Cx3cr1*$^{GFP/GFP}$ P22 male mice as a measure of synaptic status. Over- or under-pruning of synapses by dysregulated microglia have been suggested as a possible contributing factor for the altered behavior and brain sizes found in neurodevelopmental disorders (Courchesne et al., 2003; Inta et al., 2017; Lee et al., 2017; Morgan et al., 2010; Whitelaw, 2018). Here, we observed increased expression of PSD-95 in the cortices of *Cx3cr1*$^{GFP/+}$ MMD offspring and a clear absence of this effect in *Cx3cr1*$^{GFP/GFP}$ MMD knockout offspring (Fig. 6C–E). Thus, our results demonstrate offspring reared under MMD conditions developed atypical behavioral outcomes due to dysfunction of the Cx3cr1 signaling pathway and impaired synaptic modeling.

3. Discussion

Neurodevelopmental disorders represent rapidly increasing maladies worldwide (Boyle et al., 2011). While their etiology remains ill-defined, the gut microbiome is gaining attention as having a pervasive influence with far reaching consequences (Kinross et al., 2011). The current study demonstrates that antibiotics-driven, maternal microbiome dysbiosis (MMD) impairs proper neurobehavioral development, enhances PSD-95 expression, and induces a dysregulated state in microglia of the prefrontal and parietal cortices. Moreover, MMD resulted in the overexpression of Cx3cr1 on microglia, which correlated with increased expression of senescence-associated genes *Il1β* and *Trp53*. In contrast, these outcomes were significantly attenuated in pups born to dams colonized with a commensal bacterium (*L. murinus* HU-1) either during the MMD duration or at parturition suggesting these deficits may be rescued postnatally via oral gavage. We further demonstrate that MMD-induced impairments can also be rescued using *Cx3cr1*$^{GFP/GFP}$ knockout mice. These findings provide novel insight into the role that gut microbiota play in social development and suggest that microglia may be pivotal in the gut-brain axis during development through yet unexplored bacteria-derived signals.

The social preference index at P21 utilized in this study is a well-characterized behavioral assay for autism-like social deficit (Silverman et al., 2010) and served to emphasize aberrant behavioral outcomes in offspring as a result of experimental MMD. Albeit arguably less utilized in studies of neurodevelopmental disorders due to challenges posed by requisite testing of neonatal mice, the righting reflex test at P1 and cliff aversion and negative geotaxis tests at P11 parallel oligodendrocyte maturation at P1-3 and peak gliogenesis at P7-10, respectively, and are reflective of appropriate murine sensorimotor and reflexive developmental milestones (Feather-Schussler and Ferguson, 2016; Semple et al., 2013; Wu et al., 1997). Indeed, we observed transient inability to perform these tasks in MMD pups, as portrayed by recovery of P1 righting reflex deficit (Fig. 2D) at P11 (Fig. 2H) and recovery of cliff aversion/negative geotaxis deficits at P11 (Fig. 2F and G) by weaning at

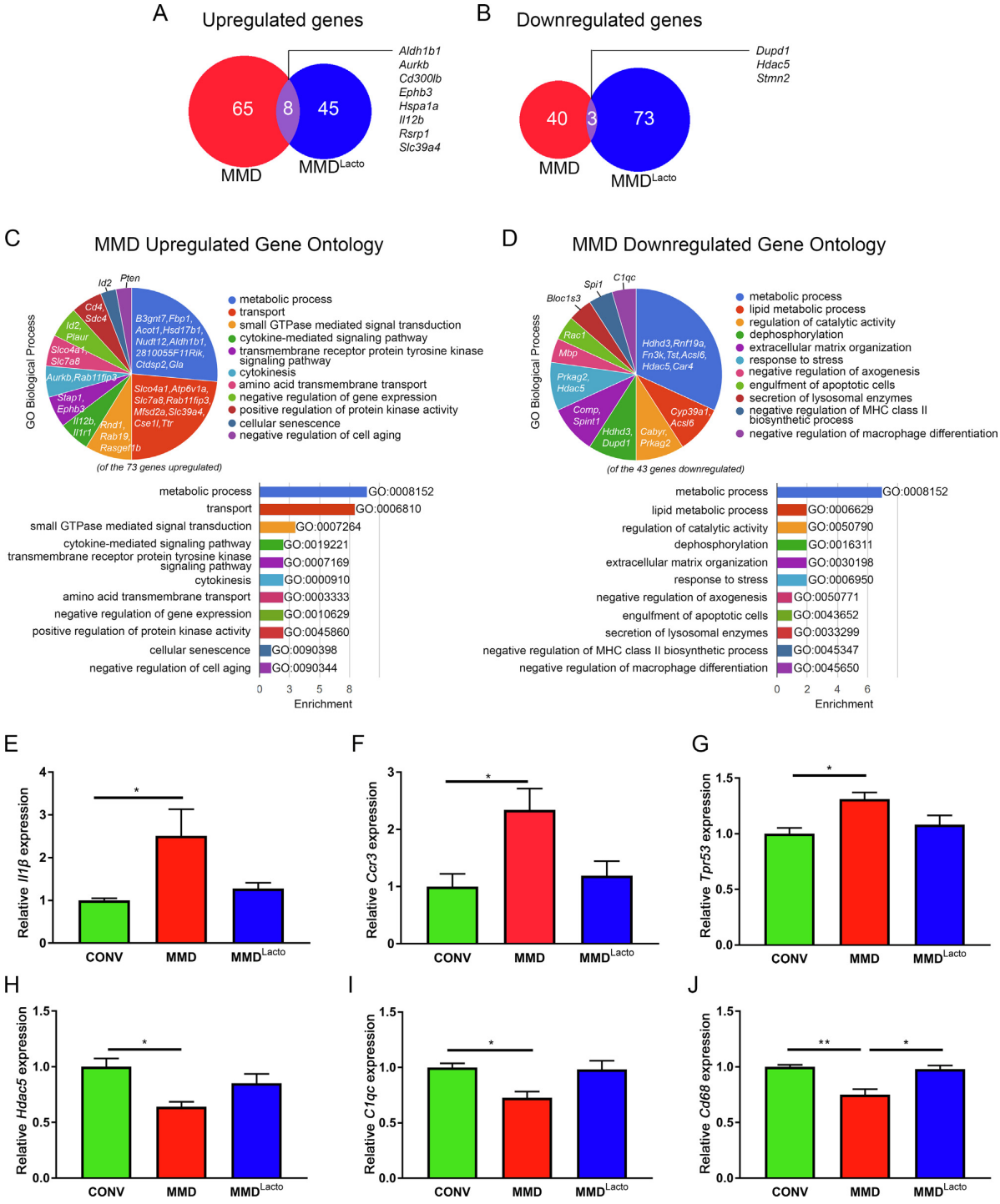

Fig. 4. Gene expression changes in cortical microglia of MMD male offspring. (A) Venn diagram of upregulated genes in MMD and MMD^{Lacto} microglia compared to CONV. (B) Venn diagram of downregulated genes in MMD and MMD^{Lacto} microglia compared to CONV. (C-D) Gene ontology enrichment analysis indicates a variety of biological processes represented by upregulated genes (C) and downregulated genes (D) with the majority of observed to be related to metabolic and cell cycle processes. (E-J) Validation of targeted genes relevant to microglia inflammation, reactivity and cellular survival, senescence by qPCR. *P $<$ 0.05 and **P $<$ 0.05.

P21 (Fig. 2J and K). It is unclear why MMD conditions prompted these developmental delays, although previous studies of germ-free mice suggested altered myelination compared to conventional controls (Hoban et al., 2016). Notably, the delayed motor skills discovered in our study reflect a growing body of clinical evidence that argues gross motor delays in infancy may serve as an early predictor of autism spectrum disorders (ASD) (Bedford et al., 2016; Bhat et al., 2012; Harris, 2017; LeBarton and Landa, 2019). Furthermore, the restoration of typical behavior in offspring reared by MMD dams supplemented with antibiotic-resistant *L. murinus* HU-1 (MMD^{Lacto}) served to prove

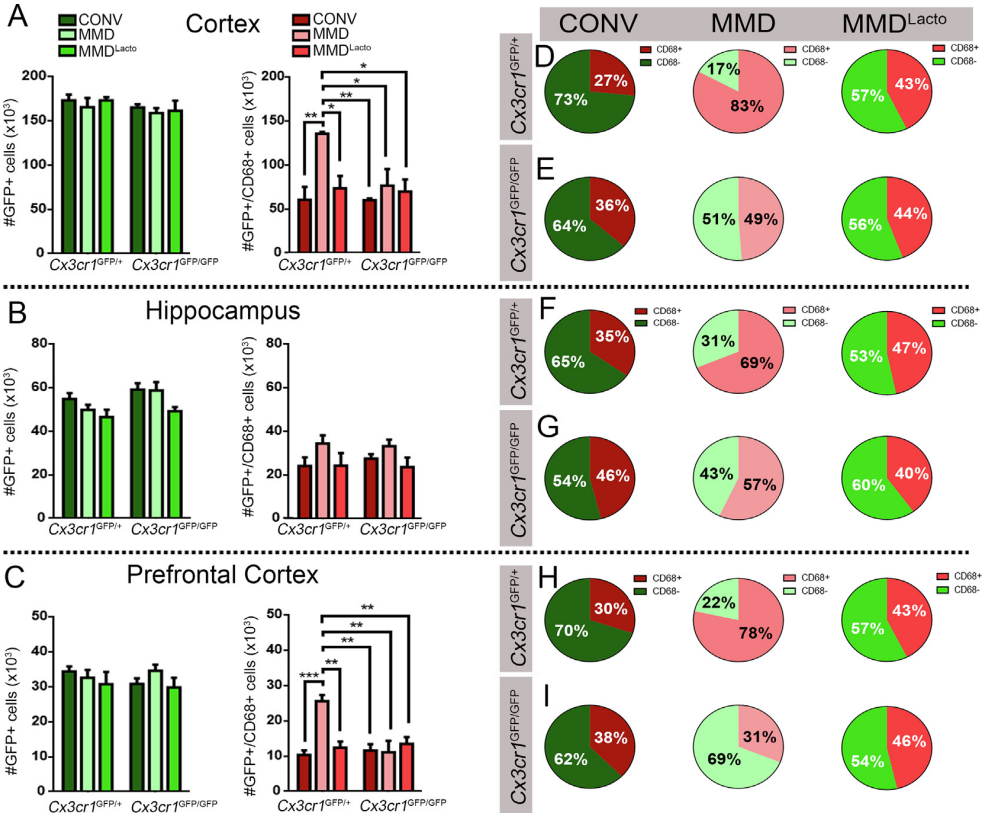

Fig. 5. MMD-induced microglial CD68-immunoreactivity is attenuated in the absence of *Cx3cr1* and in MMD^{Lacto}. (A-C) Non-biased stereological analysis of the estimated total number of GFP^+ and double-labeled $CD68^+/GFP^+$ cells in the parietal cortex, hippocampus, and prefrontal cortex of P22 male offspring. While no difference in the total microglia numbers regardless of genotype or treatment was found, the co-labeled $CD68^+/GFP^+$ cells were increased in the cortex and prefrontal cortex but not hippocampus of heterozygous MMD offspring only. Subregions of the hippocampus were analyzed as a single unit. (D-I) Pie charts organized by brain region and genotype representing the average proportion of $CD68^+/GFP^+$ versus $CD68^-/GFP^+$ cells (n = 4 litters). *P < 0.05, **P < 0.05, and ***P < 0.001.

that certain gut bacterial communities are sufficient to enable typical neurobehavioral development despite overall dysbiotic conditions during pregnancy. Indeed, numerous adult animal studies have demonstrated improvements in sociability, stress, anxiety, and depression-related behaviors following probiotic treatment (Buffington et al., 2016; Desbonnet et al., 2015; Wang et al., 2015). Here, we also demonstrate that such rescue occurs under a developmental setting.

Interestingly, we did not find the same rescue effect when dams were passively placed into conventional housing at parturition (MMD^{CONV}). This is not surprising, as fecal analysis in this group did not show the re-emergence of *Lactobacillus* until 60 days following re-conventionalization compared to 3 days following oral gavage in $MMD^{CONV+Lacto}$. *L. murinus*, in particular, is a member of the Altered Schaedler Flora, which is a collection of eight commensal gut bacteria deemed to be necessary for laboratory rodent health and further serves to underscore the likely developmental importance of *Lactobacilli* presence in maternal microbiota (Dewhirst et al., 1999; Schaedler et al., 1965; Wymore Brand et al., 2015). Accordingly, the lack of an additional control group, $CONV^{Lacto}$, in this study is due to the endemic nature of *L. murinus* in conventionally-housed mice, as well as evidence from previous studies suggesting difficulties in discerning purported benefits of probiotics under non-pathological conditions (Bravo et al., 2011; Kelly et al., 2015).

The notion of a "window of susceptibility" in the early postnatal period was demonstrated using germ-free mice, which showed reduced brain-derived neurotrophic factor, norepinephrine and serotonin levels in the cortex that could be reversed with probiotic treatment or partially restored with re-conventionalization if conducted within six weeks of birth (Sudo, 2006; Sudo et al., 2004). Although we captured longitudinal changes in behavior from birth through weaning, future studies should consider introducing treatments at various time points to better define critical periods in postnatal neurodevelopment that may be susceptible to MMD conditions and whether *L. murinus* HU-1 can prevent atypical outcomes. Nevertheless, our behavioral findings comport with these previous studies and further highlight the potential benefit of concurrent probiotic use during episodes of gut microbiome disruption in pregnancy or in early childhood development.

While the mechanism(s) by which microbiota dysbiosis impairs the development of typical social behavior remains unclear, our findings uncover a dysfunctional microglia phenotype under MMD conditions that correlates with increased PSD-95 expression and social deficits. MMD microglia show increased Cx3cr1 and CD68 protein expression, which is attenuated in the presence of *L. murinus* HU-1. Postmortem tissue analysis of autistic brains previously identified increased CD68 expression, as well as other indicators of activated microglia and neuroinflammation, in the cortex and prefrontal cortex that were paradoxically accompanied by overgrowth of grey and white matter (Courchesne et al., 2003; Lee et al., 2017; Morgan et al., 2010; Vargas et al., 2005). This correlation has lent support for the hypothesis that aberrantly activated microglia fail to regulate proper growth and pruning of neural circuitry in ASD (Matta et al., 2019). Indeed, the concept of hyperactivated microglia that fail to phagocytose has been described in neurodegenerative disorders wherein Cx3cr1 signaling mediates this phenotype in which microglia ineffectively surround

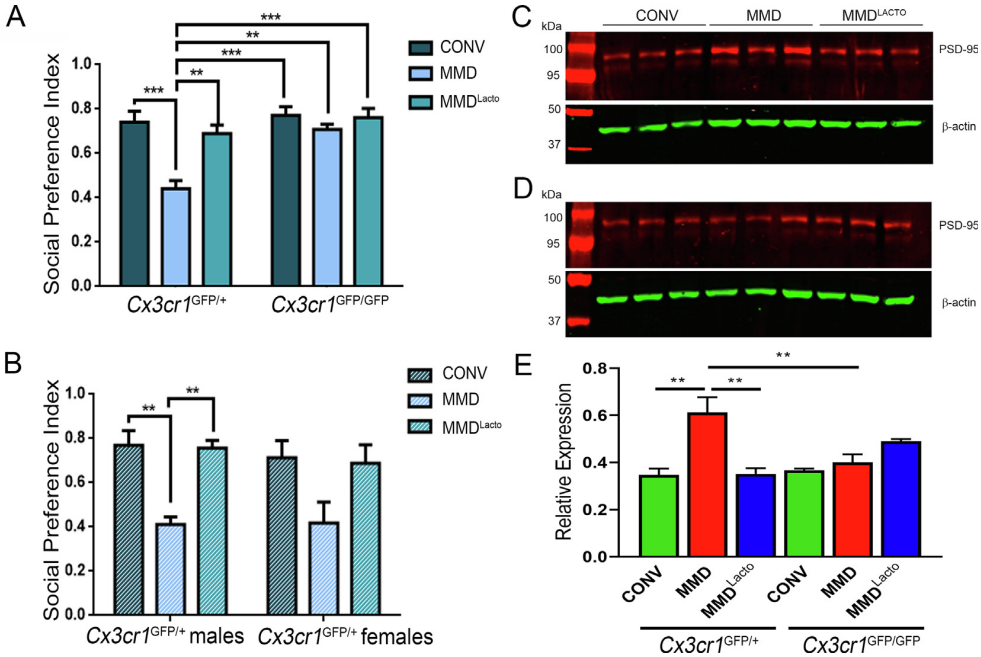

Fig. 6. Loss of *Cx3cr1* attenuates MMD-induced social deficits and PSD-95 expression. (A) Heterozygous *Cx3cr1*$^{GFP/+}$ MMD offspring exhibit social deficits at P21 compared to heterozygous CONV and MMD^{Lacto} offspring. These deficits reach significance in males, however, lack of social preference was reflected in both MMD males and females and no significant interaction was found between sex and treatment. Importantly, social deficits were attenuated in *Cx3cr1*$^{GFP/GFP}$ knockout MMD offspring. MMD^{Lacto} mice showed no social deficits regardless of genotype. (C) PSD-95 protein expression in *Cx3cr1*$^{GFP/+}$ or (D) *Cx3cr1*$^{GFP/GFP}$ cortices of male offspring (n = 3 per group). (E) Quantification of PSD-95 expression shows increased levels in MMD offspring in the presence of functional *Cx3cr1* only. (n = 4–5 litters, average 29–30 pups per group). **P < 0.05 and ***P < 0.001.

amyloid-beta plaques in lieu of phagocytosis; in contrast, deletion of the *Cx3cr1* permitted more efficient phagocytosis and function (Liu et al., 2010). Our data suggest that MMD may lead to an aberrant microglial phenotype in specific brain regions of the offspring that are directly regulated by gut signals to prevent appropriate modeling of synapses, and that this effect is mediated through Cx3cr1 signaling pathway.

Besides increased CD68 expression, we did not find additional evidence of overzealous neuroinflammation under MMD conditions. Unlike studies on maternal immune activation and age-related neuroinflammation, our cytokine profiling of maternal serum and offspring gut (cecal contents) in MMD-treated animals did not reveal elevated levels of pro-inflammatory markers, such as *Il6* and *Il17a*, compared to controls (data not shown). Nor did RNAseq analysis of cortical microglia from MMD offspring reveal a particularly pro- or anti-inflammatory phenotype with the exception of *Il12b* upregulation and *C1qc* downregulation. Our qPCR findings show *Il1β* was also increased, which is a known inflammatory cytokine as well as a key mediator cell senescence. Combined with the observed increase in *Trp53*, this suggests MMD microglia display a senescent phenotype. MMD microglia also showed greater expression of genes related to stress-induced premature senescence, such as *Sirt1*, *Wnt16*, and *Mapkapk5*, while MMD^{Lacto} microglia showed greater expression of *Sumf1, Steap3, Prkag2,* and *Spi1* that relate to processes which mitigate cellular stress, such as oxidoreductase activity, DNA repair, and apoptosis. Microglial senescence has been linked to lysosomal inclusions and immune dysfunction because of age-related myelin degradation (Safaiyan et al., 2016). Age-based microglial senescence is often cause by radical-mediated oxidative damage, whereas premature microglial senescence is said to be associated with cellular stress (Streit et al., 2014). Both types of senescent microglia are characterized by dystrophic morphology consisting of deramified and fragmented appearance, similar to our MMD microglia (Streit, 2006). Our findings suggest that MMD may permit a premature senescence-like state in microglia, however, additional studies are needed to identify the underlying mechanisms.

It remains unclear how the presence of *L. murinus* HU-1 in the gut of MMD^{Lacto} dams rescued neurobehavioral and microglial dysfunction in offspring. Recent studies on the gut-brain axis suggest several potential modes of influence, including microbial signaling via the vagus nerve and the production of microbe-derived neuroactive molecules. While we observed a significant loss of fecal SCFAs metabolites following MMD, these levels did not restore in the presence of *L. murinus* HU-1 suggesting the effects of MMD is unlikely to be metabolite-driven. We did identify, using a multiplex cytokine profiler, an upregulation of Ccl21, CRP, Cystatin C, Endostatin, and Reg3G in the cecum of the P21 MMD offspring, which was attenuated in MMD^{Lacto} pups (Supplemental Fig. 6). Moreover, several recent findings implicate the interactions between gut *Lactobacillus* and the vagus nerve in the regulation of brain regions that may affect social behavior. Bravo et al., described ameliorative effects of *L. rhamnosus* JB-1 in a mouse model of anxiety and depression that corresponded with alterations in GABA receptor gene expression in the prefrontal cortex and amygdala (Bravo et al., 2011). They found this anxiolytic and antidepressant effect was attenuated in vagotomized mice (Bravo et al., 2011). Sgritta et al., also recently demonstrated reversal of social deficits through *L. reuteri* treatment across multiple adult mouse models of ASD, which was attenuated in oxytocin receptor-deficient and vagotomized mice (Sgritta et al., 2019). Combined with our findings, these data suggest the presence of *Lactobacillus* sp. in the gut could play a critical role in modulating social behavior as well as microglial function by influencing the communication between afferent vagal nerve inputs and social reward circuits. However, additional studies are needed to evaluate Cx3cr1 expression and the microglial response to vagotomy following MMD in the presence and absence of *L. murinus* HU-1.

In conclusion, our findings describe a new model of maternal gut dysbiosis that results in atypical social development in offspring, which can be rescued by *L. murinus* HU-1 or loss of *Cx3cr1*. The current study

suggests MMD-induced behavioral outcomes may result from premature senescence of microglia that could influence synaptic pruning in regions of the brain that regulate social preference. Future studies aimed at identifying the mechanisms by which gut *Lactobacillus* communicates with the social reward center of the brain will advance our understanding and treatment of neurodevelopmental disorders.

4. Materials and methods

4.1. Animals

All mice were housed in an AAALAC accredited, virus/specific antigen-free facility with a 12 h light-dark cycle; food (Teklad 2918) and water provided *ad libitum*. Outbred CD-1 IGS mice were purchased from Charles River (Strain code 022), and inbred C57BL/6J (Stock no. 000664) and B6.129P-*Cx3cr1*^{tm1Litt}/J mice (Stock no. 005582) were purchased from Jackson Laboratory. Heterozygous *Cx3cr1*$^{GFP/+}$ mice were bred using C57BL/6J males and B6.129P-*Cx3cr1*^{tm1Litt}/J females. Homozygous *Cx3cr1*$^{GFP/GFP}$ mice were bred using B6.129P-*Cx3cr1*^{tm1Litt}/J males and females, as described (Jung et al., 2000). Breeding pairs (n = 4–6) for all strains were 6–8 weeks old and females were used to generate one litter only to prevent potential confounding generational effects in the offspring. All experiments were conducted in accordance with the NIH Guide for the Care and Use of Laboratory Animals and conducted under the approval of the Virginia Tech Institutional Animal Care and Use Committee (IACUC; #17-043).

4.2. Maternal microbiome dysbiosis (MMD) protocol

Mice were either administered an antibiotic cocktail (MMD), given a single oral dose of *Lactobacillus murinus* strain HU-1 (10^9 CFU) followed by an antibiotic cocktail (MMD^{Lacto}), or water (CONV) to establish conditions of MMD, MMD plus probiotic, and conventional housing conditions, respectively. Antibiotic cocktail of 0.4 mg/ml kanamycin, 850 U/ml colistin, 0.215 mg/ml metronidazole (Bio-World, Dublin, OH), 0.035 mg/ml gentamicin (Vet One, Boise, ID), and 0.045 mg/ml vancomycin (Hospira Inc., Lake Forest, IL) was based on a previous protocol using clinically-relevant drug dosages (Chen et al., 2008), with the addition of 0.5 mg/ml amoxicillin/clavulanic acid (Zoetis, Parsippany, NJ). Antibiotics were administered via drinking water to treatment groups one week prior to breeding and maintained throughout the duration of the experiment until sacrifice at pup weaning (P22). MMD^{Lacto} mice received a single, oral gavage of a novel, lab-generated strain of *L. murinus* HU-1 three days prior to beginning the antibiotic cocktail. Re-conventionalization experiments were conducted by moving MMD dams to dirtied conventional housing near parturition (approx. ~E19-21) to replenish their gut microbiota via coprophagic behavior (MMD^{CONV}). Additional MMD dams were also re-conventionalized in this fashion and given an oral dose of *L. murinus* HU-1 to ensure colonization with this specific bacterium (MMD$^{CONV+Lacto}$). MMD conditions were confirmed via PCR testing of fecal DNA for 16s rRNA (8F forward 5′-AGAGTTTGATCCTGGCTCAG-3′ and U1429 reverse 5′-ACGGTTACCTTGTTACGACTT-3′) and *L. murinus* (forward 5′-GCAATGATGCGTAGCCGAAC-3′ and reverse 5′-GCACTTTCTTCTCT AACAACAGGG-3′) prior to breeding, during gestation, and in the offspring near weaning (P18-21).

4.3. Microbiome profiling

Fresh fecal pellets from dams were cultured on BHI, MacConkey, and MRS agar (Becton, Dickinson and Company, Franklin Lakes, NJ). Fecal cultures from experimental breeders using rich media agar plates revealed numerous and diverse colony formations from CONV dams, monocolonization by *L. murinus* HU-1 only from MMD^{Lacto} dams (confirmed by MALDI-TOF), and no growth from MMD dams (data not shown). Additional culture plates were used to confirm antibiotic resistance in *L. murinus* HU-1 by Kirby-Bauer testing. Fecal DNA was extracted via kit (SKU D6010, Zymo Research, Irvine, CA) and submitted to Argonne National Laboratory for 16s rRNA sequencing using Illumina MiSeq.

4.4. Behavioral assays

Individual offspring were tested at P1, P11, and P21 against milestones of typical behavioral development in motor-reflexive tasks: righting—ability to re-orient body on all four paws after being placed on back; cliff aversion—ability to stop from falling off a surface edge; and negative geotaxis—ability to orient body upwards when placed head-down at a steep angle, as described (Wu et al., 1997). Each test was repeated 4 times and scored as a percentage of successful attempts with 100% indicating proper motor-reflexive development and 0% indicating poor motor-reflexive development. Weanling pups (P21) were tested additionally for social preference via the three-chamber social test, as described (Silverman et al., 2010); behavior was recorded and quantified by EthoVision XT software (Noldus, Leesburg, VA). Briefly, individual pups from a litter were allowed to habituate inside a three-chambered box for 10 min before the 10-minute testing period in which the pup was observed for interactions with a social and non-social stimulus that were placed in the outer chambers. Age, sex, and strain-matched mice were used as the social stimulus and a green plastic block was used as the non-social stimulus. Social preference was scored as time spent with the social stimulus divided by total time spent with both social and non-social stimuli such that a score of 1.0 indicates highest social preference and 0.0 indicates lowest social preference. Significant interaction between sex and treatment were not found, therefore, both male and female pups were tested. All individual behavior scores were averaged for each litter and represented as n = 1.

4.5. Fecal metabolite analysis

Fresh fecal pellets from pregnant dams were collected directly into individual 1.5 ml centrifuge tubes and weighed, and homogenized with 1 ml of deionized water. The tubes were allowed to settle at room temperature for 2 h and then submitted to Virginia Tech Environmental and Water Resources Research Facility for quantification of various volatile fatty acids via Hewlett-Packard 5890 gas chromatograph fitted with a flame ionization detector (GC-FID) coupled with a Nukol GC column and a Hewlett-Packard 7673 GC/SFC injector.

4.6. Tissue processing and staining

Brains from male offspring were collected at P22, perfused with 10% formalin, cryopreserved overnight in 20% sucrose and then frozen in OCT compound (Fisher Scientific, Hampton, NH). Whole brains were processed on a cryostat (CryoStar NX50 Cryostat) into 30 μM coronal serial sections spaced 10 sections apart with 5 sections per slide and each section 300 μM apart. Tissue sections were stored in −80 °C until use. Sections were fixed with 10% formalin for 10 min followed by 3x washed with 1X PBS then blocked in 2% fish gelatin and 0.2% Triton X-100 (Sigma-Aldrich, St. Louis, MO) for 1 h at room temperature. Primary antibodies (CD68 Cat. #MA5-16674, Invitrogen, Carlsbad, CA; Neurofilament Cat. # MAB1621, Chemicon International, Temecula, CA; Cx3cr1 Cat. #Ab8021 Abcam, Cambridge, MA) were diluted in block and was applied to each individual slide at 1:200 dilution and incubated overnight in 4 °C. The following day, sections were washed in 1X PBS before application of secondary antibody for 1.5–2 h at room temperature (1X PBS solution with secondary antibody 1:500 donkey anti-rat Alexa-Fluor 594, Invitrogen Cat. #A-21209, Carlsbad, CA). The sections were washed with 1X PBS before prior to mounting in DAPI Fluoromount-G (Southern Biotech, Birmingham, AL). Cortical mantle thickness was determined using Nissl-stained slides using cresyl violet acetate 2.5% solution (Electron Microscopy Science, Hatfield, PA), as

described previously (Brickler et al., 2018). Thickness was averaged from three measurements of the cortical layer spanning from the dorsal corpus callosum to the meninges and measured across five serial coronal sections from approx. −1.38 to −2.58 mm from bregma (n = 4).

4.7. Stereological and confocal image analyses

Cell counts for the hippocampus (HPC), cortex (CTX), and prefrontal cortex (PFC) of *Cx3cr1*$^{GFP/+}$ and *Cx3cr1*$^{GFP/GFP}$ male offspring were assessed by a blinded investigator using Optical Fractionator from StereoInvestigator (MicroBrightField, Williston, VT) and an upright Olympus BX51TRF motorized microscope (Olympus America, Center Valley, PA). Grid size was set at 300 × 300 mm with a 75 × 75 mm counting frame for HPC and PFC, and 700 × 700 mm with a 300 × 300 mm counting frame for CTX. HPC and CTX regions were estimated to be located at approx. −1.38 to −2.58 mm A/P bregma and PFC regions at approx. 1.82 to 0.62 mm A/P bregma per Allen Mouse Brain Atlas (Lein et al., 2007). Subregions of the hippocampus were analyzed as a single unit. The right hemisphere consisted of 5 coronal serial sections. Confocal images were obtained using an inverted Zeiss 880 (Carl Zeiss AG, Oberkochen, Germany).

4.8. Proteome profiling and western blotting

To identify cytokine levels in the gut, protein was isolated from 100 mg of cecal content from male offspring at P22, as described (Dillenburg-Pilla et al., 2016), for measurement via Proteome Profiler Mouse XL Cytokine Array (R&D Systems, Minneapolis, MN) per manufacturer's instructions. To identify protein levels in the cortex, dissected cortices from P22 male offspring were lysed in RIPA buffer (Tris-base 50 mM, NaCl 150 mM, EDTA 1 mM, NP-40 1%, Sodium deoxycholate 0.25%, NaF 20 mM, 1 mM Na3VO4 1 mM, β-glycerophosphate 10 mM, Azide 0.02%) with Roche Proteinase Inhibitor Cocktail (Cat. # 25178600, Indianapolis, IN) and Thermo Fisher Scientific Pierce™ Phosphatase Inhibitors (Catalog # 88667, Waltham, MA), aliquoted and kept in −80 °C until use. The total amount of protein was quantified by Lowry method (Bio-Rad, Hercules, CA). 50 µg total protein of each sample was separated by 8% SDS-PAGE, then blotted on to Immin-Blot™ PVDF membrane (Bio-Rad, Hercules, CA). Membranes were incubated with primary antibodies (PSD-95 Cat. #3450, Cell Signaling, Danvers, MA; beta-actin Cat. #3700, Cell Signaling, Danvers, MA) in blocking solution: TBS/0.1% Tween20 (TBST)/5% bovine serum albumin (BSA) for overnight at 4 °C, washed 4× with TBST, and incubated with secondary antibodies (anti-rabbit IgG Dylight™ conjugate 680 or anti-mouse IgG Dylight™ conjugate 800; Cell Signaling Technology, Danvers, MA) for 2 h in blocking solution at room temperature. Following 4× wash with TBST, images were acquired by using LI-COR Odyssey Imaging Systems (LI-COR, Inc), and band intensities were quantified by using NIH ImageJ software.

4.9. RNA sequencing and analysis

Whole cortex was dissected from brains of *Cx3cr1*$^{GFP/+}$ male offspring at P22, placed in Leibovitz's L-15 dissecting media on ice (ThermoFisher, Waltham, MA), subjected to neural dissociation (Kit from Miltenyi Biotec, Auburn, CA), and placed in FACS buffer (PBS, 5% FBS, 0.1% Sodium azide). Two brains were pooled for each individual isolation per experimental group. Each group consisted of three biological triplicates. GFP$^+$ cells were then collected via flow cytometry (BD FACS Aria, San Jose, CA). Total RNA was isolated from sorted cells using TRIzol® reagent (Life Technologies, Carlsbad, CA) per manufacturer's instructions. RNA quantification was carried out by measuring absorbance with spectrophotometer ND-1000 (NanoDrop). Isolated RNA was submitted to BGI Americas Corp. (Cambridge, MA) for RNA quantification sequencing using Illumina platform. Fragments per kilobase of transcript per million reads (FPKM) values were calculated for each gene useGalaxy.org and Cufflinks software (version 2.2.1). Significant changes were calculated using Cuffdiff (version 2.2.1) and normalized using geometric method. Files were then passed to the Cummerbund, an R Core Team package https://www.R-project.org/ version 3.1.2 to determine the significantly differentially expressed genes (FDR < 0.05). Gene ontology (GO) biological processes of significantly upregulated and downregulated genes were conducted via GeneCodis version 3.0 (Carmona-Saez et al., 2007; Nogales-Cadenas et al., 2009; Tabas-Madrid et al., 2012) and PANTHER version 14 enrichment analysis tools (Mi et al., 2019).

4.10. qPCR

RNA was reverse transcribed into cDNA with iScript™ cDNA synthesis kit (Bio-Rad, Hercules, CA) per manufacturer's specifications. For qRT-PCR analysis, 50 ng cDNA per reaction was amplified using iTaq™ Universal SYBR® Green Supermix (Bio-Rad, Hercules, CA). Expression changes were calculated using ΔCq values with reference to *β-actin* internal control gene. Relative expression was calculated then normalized and compared to appropriate treated or control samples. All primers were designed to span exon junctions and were tested for primer efficiency which ranged from 87 to 110% prior to use.

Gene	Primer sequence (5′–3′)
β-actin	Fw: TCGTACCACAGGCATTGTGAT GGA
	Rv: TGATGTCACGCACGATTTCCCTCT
C1qc	Fw: TAGGGCCAGAAGAAACAGCA
	Rv: AGGCCTGAAGTCCCTTACAC
Ccr3	Fw: ACTGGACTCATAAAGGACTTA GCA
	Rv: GTGCCCACTCATATTCATAGGG
Cd68	Fw: TCACCTTGACCTGCTCTCTCT
	Rv: GGACCAGGCCAATGATGAGA
Hdac5	Fw: AACAGAGCACGCTCATAGCA
	Rv: GGTGCCTCGGGAGCTTAC
Il1β	Fw: TGTGTAATGAAAGACGGCACAC
	Rv: CCATCTTCTTCTTTGGGTATTGCT
Trp53	Fw: CAGTCTGGGACAGCCAAGTC
	Rv: CCAGCTGGCAGAATAGCTTA

4.11. Statistics

Data were graphed using Prism software (Version 7, GraphPad, San Diego, CA). Student's unpaired two-tailed *t* test was used for comparison of two experimental groups. For three or more groups, multiple comparisons were done using one-way and two-way ANOVA where appropriate, followed by Tukey's multiple comparisons test or Bonferroni where appropriate. Changes were identified as significant at $p < 0.05$. Mean values were reported together with the SEM.

Author contribution

Y.L., E.A.K., X.W., E.K.G., W.M., C.K., M.L., V.M., R.W., M.C., A.H., T.H., and M.H.T. performed research and analyzed data. Y.L. wrote paper. M.H.T. wrote and edited paper, designed research, and contributed reagents/analytic tools.

Declaration of Competing Interest

The authors declare that they have no known competing financial interests or personal relationships that could have appeared to influence the work reported in this paper.

Acknowledgments

This work was supported by the Center for One Health Research at

Virginia Maryland College of Veterinary Medicine and The Edward Via College of Osteopathic Medicine (MHT), Virginia Tech Center for Autism Research Student Award (YL), and Virginia Tech Graduate Research Development Program Award (YL). YL was one of the 2017-2018 award recipients of the Danone North America Gut Microbiome, Yogurt and Probiotics Fellowship Grant. We thank Ryan McMillan at the Virginia Tech Metabolomic Phenotyping Core, Elizabeth Smiley at Virginia Tech Environmental and Water Resources Research Facility, Virginia Tech Animal Laboratory Services, and Melissa Makris at VMCVM Flow Cytometry Lab for their services in support of this research.

Appendix A. Supplementary data

Supplementary data to this article can be found online at https://doi.org/10.1016/j.bbi.2019.07.025.

References

Al-Haddad, B.J.S., Jacobsson, B., Chabra, S., Modzelewska, D., Olson, E.M., Bernier, R., Enquobahrie, D.A., Hagberg, H., Ostling, S., Rajagopal, L., et al., 2019. Long-term risk of neuropsychiatric disease after exposure to infection in utero. JAMA Psychiatry.

Andrade, S.E., Gurwitz, J.H., Davis, R.L., Chan, K.A., Finkelstein, J.A., Fortman, K., McPhillips, H., Raebel, M.A., Roblin, D., Smith, D.H., et al., 2004. Prescription drug use in pregnancy. Am. J. Obstet. Gynecol. 191, 398–407.

Atladottir, H.O., Henriksen, T.B., Schendel, D.E., Parner, E.T., 2012. Autism after infection, febrile episodes, and antibiotic use during pregnancy: an exploratory study. Pediatrics 130, e1447–1454.

Backhed, F., Roswall, J., Peng, Y., Feng, Q., Jia, H., Kovatcheva-Datchary, P., Li, Y., Xia, Y., Xie, H., Zhong, H., et al., 2015. Dynamics and stabilization of the human gut microbiome during the first year of life. Cell Host Microbe 17, 690–703.

Bedford, R., Pickles, A., Lord, C., 2016. Early gross motor skills predict the subsequent development of language in children with autism spectrum disorder. Autism Res. 9, 993–1001.

Bhat, A.N., Galloway, J.C., Landa, R.J., 2012. Relation between early motor delay and later communication delay in infants at risk for autism. Infant Behav. Dev. 35, 838–846.

Boyle, C.A., Boulet, S., Schieve, L.A., Cohen, R.A., Blumberg, S.J., Yeargin-Allsopp, M., Visser, S., Kogan, M.D., 2011. Trends in the prevalence of developmental disabilities in US children, 1997–2008. Pediatrics 127, 1034–1042.

Braniste, V., Al-Asmakh, M., Kowal, C., Anuar, F., Abbaspour, A., Toth, M., Korecka, A., Bakocevic, N., Ng, L.G., Kundu, P., et al., 2014. The gut microbiota influences blood-brain barrier permeability in mice. Sci. Transl. Med. 6, 263ra158.

Bravo, J.A., Forsythe, P., Chew, M.V., Escaravage, E., Savignac, H.M., Dinan, T.G., Bienenstock, J., Cryan, J.F., 2011. Ingestion of Lactobacillus strain regulates emotional behavior and central GABA receptor expression in a mouse via the vagus nerve. Proc. Natl. Acad. Sci. U.S.A. 108, 16050–16055.

Brickler, T.R., Hazy, A., Guilhaume Correa, F., Dai, R., Kowalski, E.J.A., Dickerson, R., Chen, J., Wang, X., Morton, P.D., Whittington, A., et al., 2018. Angiopoietin/Tie2 axis regulates the age-at-injury cerebrovascular response to traumatic brain injury. J. Neurosci. 38, 9618–9634.

Buffington, S.A., Di Prisco, G.V., Auchtung, T.A., Ajami, N.J., Petrosino, J.F., Costa-Mattioli, M., 2016. Microbial reconstitution reverses maternal diet-induced social and synaptic deficits in offspring. Cell 165, 1762–1775.

Carmona-Saez, P., Chagoyen, M., Tirado, F., Carazo, J.M., Pascual-Montano, A., 2007. GENECODIS: a web-based tool for finding significant concurrent annotations in gene lists. Genome Biol. 8, R3.

Chen, X., Katchar, K., Goldsmith, J.D., Nanthakumar, N., Cheknis, A., Gerding, D.N., Kelly, C.P., 2008. A mouse model of Clostridium difficile-associated disease. Gastroenterology 135, 1984–1992.

Chen, V.S., Morrison, J.P., Southwell, M.F., Foley, J.F., Bolon, B., Elmore, S.A., 2017. Histology atlas of the developing prenatal and postnatal mouse central nervous system, with emphasis on prenatal days E7.5 to E18.5. Toxicol. Pathol. 45, 705–744.

Chistiakov, D.A., Killingsworth, M.C., Myasoedova, V.A., Orekhov, A.N., Bobryshev, Y.V., 2017. CD68/macrosialin: not just a histochemical marker. Lab Invest. 97, 4–13.

Choi, G.B., Yim, Y.S., Wong, H., Kim, S., Kim, H., Kim, S.V., Hoeffer, C.A., Littman, D.R., Huh, J.R., 2016. The maternal interleukin-17a pathway in mice promotes autism-like phenotypes in offspring. Science 351, 933–939.

Courchesne, E., Carper, R., Akshoomoff, N., 2003. Evidence of brain overgrowth in the first year of life in autism. Jama 290, 337–344.

Desbonnet, L., Clarke, G., Traplin, A., O'Sullivan, O., Crispie, F., Moloney, R.D., 2015. Gut microbiota depletion from early adolescence in mice: implications for brain and behaviour. Brain Behav. Immun. 48, 165–173.

Dewhirst, F.E., Chien, C.C., Paster, B.J., Ericson, R.L., Orcutt, R.P., Schauer, D.B., Fox, J.G., 1999. Phylogeny of the defined murine microbiota: altered Schaedler flora. Appl. Environ. Microbiol. 65, 3287–3292.

Diaz Heijtz, R., Wang, S., Anuar, F., Qian, Y., Bjorkholm, B., Samuelsson, A., Hibberd, M.L., Forssberg, H., Pettersson, S., 2011. Normal gut microbiota modulates brain development and behavior. Proc. Natl. Acad. Sci. U.S.A. 108, 3047–3052.

Dillenburg-Pilla, P., Zarate-Blades, C.R., Silver, P.B., Horai, R., Caspi, R.R., 2016. Preparation of protein-containing extracts from microbiota-rich intestinal contents. Bio Protoc. 6, e1936.

Dorfman, M.D., Krull, J.E., Douglass, J.D., Fasnacht, R., Lara-Lince, F., Meek, T.H., Shi, X., Damian, V., Nguyen, H.T., Matsen, M.E., et al., 2017. Sex differences in microglial CX3CR1 signalling determine obesity susceptibility in mice. Nat. Commun. 8, 14556.

Edmonson, C., Ziats, M.N., Rennert, O.M., 2014. Altered glial marker expression in autistic post-mortem prefrontal cortex and cerebellum. Mol. Autism 5, 3.

Erny, D., Hrabe de Angelis, A.L., Jaitin, D., Wieghofer, P., Staszewski, O., David, E., Keren-Shaul, H., Mahlakoiv, T., Jakobshagen, K., Buch, T., et al., 2015. Host microbiota constantly control maturation and function of microglia in the CNS. Nat. Neurosci. 18, 965–977.

Erny, D., Hrabe de Angelis, A.L., Prinz, M., 2017. Communicating systems in the body: how microbiota and microglia cooperate. Immunology 150, 7–15.

Feather-Schussler, D.N., Ferguson, T.S., 2016. A battery of motor tests in a neonatal mouse model of cerebral palsy. J. Vis. Exp. 53569.

Gacias, M., Gaspari, S., Santos, P.M., Tamburini, S., Andrade, M., Zhang, F., Shen, N., Tolstikov, V., Kiebish, M.A., Dupree, J.L., et al., 2016. Microbiota-driven transcriptional changes in prefrontal cortex override genetic differences in social behavior. Elife 5, e13442.

Gardiner, G.E., Casey, P.G., Casey, G., Lynch, P.B., Lawlor, P.G., Hill, C., Fitzgerald, G.F., Stanton, C., Ross, R.P., 2004. Relative ability of orally administered Lactobacillus murinus to predominate and persist in the porcine gastrointestinal tract. Appl. Environ. Microbiol. 70, 1895–1906.

Greetham, H.L., Giffard, C., Hutson, R.A., Collins, M.D., Gibson, G.R., 2002. Bacteriology of the Labrador dog gut: a cultural and genotypic approach. J. Appl. Microbiol. 93, 640–646.

Hammond, T.R., Robinton, D., Stevens, B., 2018. Microglia and the brain: complementary partners in development and disease. Ann. Rev. Cell Dev. Biol. 34, 523–544.

Harris, S.R., 2017. Early motor delays as diagnostic clues in autism spectrum disorder. Eur. J. Pediatrics 176, 1259–1262.

Hoban, A.E., Stilling, R.M., Ryan, F.J., Shanahan, F., Dinan, T.G., Claesson, M.J., Clarke, G., Cryan, J.F., 2016. Regulation of prefrontal cortex myelination by the microbiota. Transl. Psychiatry 6, e774.

Hulsen, T., de Vlieg, J., Alkema, W., 2008. BioVenn - a web application for the comparison and visualization of biological lists using area-proportional Venn diagrams. BMC Genomics 9, 488.

Inta, D., Lang, U.E., Borgwardt, S., Meyer-Lindenberg, A., Gass, P., 2017. Microglia activation and Schizophrenia: lessons from the effects of minocycline on postnatal neurogenesis, neuronal survival and synaptic pruning. Schizophr. Bull. 43, 493–496.

Jang, H.M., Lee, H.J., Jang, S.E., Han, M.J., Kim, D.H., 2018. Evidence for interplay among antibacterial-induced gut microbiota disturbance, neuro-inflammation, and anxiety in mice. Mucosal Immunol. 11, 1386–1397.

Jiang, H.Y., Xu, L.L., Shao, L., Xia, R.M., Yu, Z.H., Ling, Z.X., Yang, F., Deng, M., Ruan, B., 2016. Maternal infection during pregnancy and risk of autism spectrum disorders: a systematic review and meta-analysis. Brain Behav. Immun. 58, 165–172.

Jung, S., Aliberti, J., Graemmel, P., Sunshine, M.J., Kreutzberg, G.W., Sher, A., Littman, D.R., 2000. Analysis of fractalkine receptor CX(3)CR1 function by targeted deletion and green fluorescent protein reporter gene insertion. Mol. Cell Biol. 20, 4106–4114.

Kelly, J.R., Kennedy, P.J., Cryan, J.F., Dinan, T.G., Clarke, G., Hyland, N.P., 2015. Breaking down the barriers: the gut microbiome, intestinal permeability and stress-related psychiatric disorders. Front. Cell Neurosci. 9, 392.

Kinross, J.M., Darzi, A.W., Nicholson, J.K., 2011. Gut microbiome-host interactions in health and disease. Genome Med. 3, 14.

Korzhevskii, D.E., Kirik, O.V., 2016. Brain microglia and microglial markers. Neurosci. Behav. Physiol. 46, 284–290.

LaSala, P.R., Segal, J., Han, F.S., Tarrand, J.J., Han, X.Y., 2007. First reported infections caused by three newly described genera in the family Xanthomonadaceae. J. Clin. Microbiol. 45, 641–644.

LeBarton, E.S., Landa, R.J., 2019. Infant motor skill predicts later expressive language and autism spectrum disorder diagnosis. Infant Behav. Dev. 54, 37–47.

Leclercq, S., Mian, F.M., Stanisz, A.M., Bindels, L.B., Cambier, E., Ben-Amram, H., Koren, O., Forsythe, P., Bienenstock, J., 2017. Low-dose penicillin in early life induces long-term changes in murine gut microbiota, brain cytokines and behavior. Nat. Commun. 8, 15062.

Lee, A.S., Azmitia, E.C., Whitaker-Azmitia, P.M., 2017. Developmental microglial priming in postmortem autism spectrum disorder temporal cortex. Brain Behav. Immun. 62, 193–202.

Lee, B.K., Magnusson, C., Gardner, R.M., Blomstrom, A., Newschaffer, C.J., Burstyn, I., Karlsson, H., Dalman, C., 2015. Maternal hospitalization with infection during pregnancy and risk of autism spectrum disorders. Brain Behav. Immun. 44, 100–105.

Lein, E.S., Hawrylycz, M.J., Ao, N., Ayres, M., Bensinger, A., Bernard, A., Boe, A.F., Boguski, M.S., Brockway, K.S., Byrnes, E.J., et al., 2007. Genome-wide atlas of gene expression in the adult mouse brain. Nature 445, 168–176.

Lenz, K.M., Nelson, L.H., 2018. Microglia and beyond: innate immune cells as regulators of brain development and behavioral function. Front. Immunol. 9, 698.

Liu, Z., Condello, C., Schain, A., Harb, R., Grutzendler, J., 2010. CX3CR1 in microglia regulates brain amyloid deposition through selective protofibrillar amyloid-beta phagocytosis. J. Neurosci. 30, 17091–17101.

Lydholm, C.N., Kohler-Forsberg, O., Nordentoft, M., Yolken, R.H., Mortensen, P.B., Petersen, L., Benros, M.E., 2019. Parental infections before, during, and after pregnancy as risk factors for mental disorders in childhood and adolescence: a nationwide danish study. Biol. Psychiatry 85, 317–325.

Matcovitch-Natan, O., Winter, D.R., Giladi, A., Vargas Aguilar, S., Spinrad, A., Sarrazin, S., Ben-Yehuda, H., David, E., Zelada Gonzalez, F., Perrin, P., et al., 2016. Microglia development follows a stepwise program to regulate brain homeostasis. Science 353, aad8670.

Matta, S.M., Hill-Yardin, E.L., Crack, P.J., 2019. The influence of neuroinflammation in Autism Spectrum Disorder. Brain Behav. Immun. 79, 75–90.
Mi, H., Muruganujan, A., Ebert, D., Huang, X., Thomas, P.D., 2019. PANTHER version 14: more genomes, a new PANTHER GO-slim and improvements in enrichment analysis tools. Nucl. Acids Res. 47, D419–D426.
Morgan, J.T., Chana, G., Pardo, C.A., Achim, C., Semendeferi, K., Buckwalter, J., Courchesne, E., Everall, I.P., 2010. Microglial activation and increased microglial density observed in the dorsolateral prefrontal cortex in autism. Biol. Psychiatry 68, 368–376.
Mortensen, P.B., Norgaard-Pedersen, B., Waltoft, B.L., Sorensen, T.L., Hougaard, D., Torrey, E.F., Yolken, R.H., 2007. Toxoplasma gondii as a risk factor for early-onset schizophrenia: analysis of filter paper blood samples obtained at birth. Biol. Psychiatry 61, 688–693.
Nogales-Cadenas, R., Carmona-Saez, P., Vazquez, M., Vicente, C., Yang, X., Tirado, F., Carazo, J.M., Pascual-Montano, A., 2009. GeneCodis: interpreting gene lists through enrichment analysis and integration of diverse biological information. Nucl. Acids Res. 37, W317–322.
Nuriel-Ohayon, M., Neuman, H., Koren, O., 2016. Microbial changes during pregnancy, birth, and infancy. Front. Microbiol. 7, 1031.
Panek, C.A., Ramos, M.V., Mejias, M.P., Abrey-Recalde, M.J., Fernandez-Brando, R.J., Gori, M.S., Salamone, G.V., Palermo, M.S., 2015. Differential expression of the fractalkine chemokine receptor (CX3CR1) in human monocytes during differentiation. Cell Mol. Immunol. 12, 669–680.
Paolicelli, R.C., Bisht, K., Tremblay, M.E., 2014. Fractalkine regulation of microglial physiology and consequences on the brain and behavior. Front. Cell Neurosci. 8, 129.
Safaiyan, S., Kannaiyan, N., Snaidero, N., Brioschi, S., Biber, K., Yona, S., Edinger, A.L., Jung, S., Rossner, M.J., Simons, M., 2016. Age-related myelin degradation burdens the clearance function of microglia during aging. Nat. Neurosci. 19, 995–998.
Sampson, T.R., Mazmanian, S.K., 2015. Control of brain development, function, and behavior by the microbiome. Cell Host Microbe 17, 565–576.
Sarma-Rupavtarm, R.B., Ge, Z., Schauer, D.B., Fox, J.G., Polz, M.F., 2004. Spatial distribution and stability of the eight microbial species of the altered schaedler flora in the mouse gastrointestinal tract. Appl. Environ. Microbiol. 70, 2791–2800.
Schaedler, R.W., Dubs, R., Costello, R., 1965. Association of germfree mice with bacteria isolated from normal mice. J. Exp. Med. 122, 77–82.
Semple, B.D., Blomgren, K., Gimlin, K., Ferriero, D.M., Noble-Haeusslein, L.J., 2013. Brain development in rodents and humans: identifying benchmarks of maturation and vulnerability to injury across species. Prog. Neurobiol. 106–107, 1–16.
Sgritta, M., Dooling, S.W., Buffington, S.A., Momin, E.N., Francis, M.B., Britton, R.A., Costa-Mattioli, M., 2019. Mechanisms underlying microbial-mediated changes in social behavior in mouse models of autism spectrum disorder. Neuron 101 (246–259), e246.
Sharon, G., Sampson, T.R., Geschwind, D.H., Mazmanian, S.K., 2016. The central nervous system and the gut microbiome. Cell 167, 915–932.
Silverman, J.L., Yang, M., Lord, C., Crawley, J.N., 2010. Behavioural phenotyping assays for mouse models of autism. Nat. Rev. Neurosci. 11, 490–502.
Smith, S.E., Li, J., Garbett, K., Mirnics, K., Patterson, P.H., 2007. Maternal immune activation alters fetal brain development through interleukin-6. J. Neurosci. 27, 10695–10702.
Streit, W.J., 2006. Microglial senescence: does the brain's immune system have an expiration date? Trends Neurosci. 29, 506–510.
Streit, W.J., Xue, Q.S., Tischer, J., Bechmann, I., 2014. Microglial pathology. Acta Neuropathol. Commun. 2, 142.
Sudo, N., 2006. Stress and gut microbiota: does postnatal microbial colonization programs the hypothalamic-pituitary-adrenal system for stress response? Int. Congress Series 1287, 350–354.
Sudo, N., Chida, Y., Aiba, Y., Sonoda, J., Oyama, N., Yu, X.N., Kubo, C., Koga, Y., 2004. Postnatal microbial colonization programs the hypothalamic-pituitary-adrenal system for stress response in mice. J. Physiol. 558, 263–275.
Tabas-Madrid, D., Nogales-Cadenas, R., Pascual-Montano, A., 2012. GeneCodis3: a non-redundant and modular enrichment analysis tool for functional genomics. Nucl. Acids Res. 40, W478–483.
Theiler, K., 1972. The House Mouse. Development and Normal Stages from Fertilization to 4 Weeks of Age. Springer-Verlag, Berlin\Heidelberg, New York.
Thion, M.S., Low, D., Silvin, A., Chen, J., Grisel, P., Schulte-Schrepping, J., Blecher, R., Ulas, T., Squarzoni, P., Hoeffel, G., et al., 2018. Microbiome influences prenatal and adult microglia in a sex-specific manner. Cell 172 (500–516), e516.
Tochitani, S., Ikeno, T., Ito, T., Sakurai, A., Yamauchi, T., Matsuzaki, H., 2016. Administration of non-absorbable antibiotics to pregnant mice to perturb the maternal gut Microbiota is associated with alterations in offspring behavior. PLoS One 11, e0138293.
Vargas, D.L., Nascimbene, C., Krishnan, C., Zimmerman, A.W., Pardo, C.A., 2005. Neuroglial activation and neuroinflammation in the brain of patients with autism. Ann. Neurol. 57, 67–81.
Vasconcelos, A.L.S., Nicoli, J.R., Nardi, R.M.D., 2003. Antagonistic and protective effects against Salmonella enterica serovar typhimurium by Lactobacillus murinus in the digestive tract of gnotobiotic mice. Braz. J. Microbiol. 34, 21–24.
Verheijden, S., De Schepper, S., Boeckxstaens, G.E., 2015. Neuron-macrophage crosstalk in the intestine: a “microglia” perspective. Front. Cell Neurosci. 9, 403.
Vuong, H.E., Yano, J.M., Fung, T.C., Hsiao, E.Y., 2017. The microbiome and host behavior. Annu. Rev. Neurosci. 40, 21–49.
Wang, T., Hu, X., Liang, S., Li, W., Wu, X., Wang, L., Jin, F., 2015. Lactobacillus fermentum NS9 restores the antibiotic induced physiological and psychological abnormalities in rats. Benef. Microbes 6, 707–717.
Whitelaw, B.S., 2018. Microglia-mediated synaptic elimination in neuronal development and disease. J. Neurophysiol. 119, 1–4.
Wong, D., Nielsen, T.B., Bonomo, R.A., Pantapalangkoor, P., Luna, B., Spellberg, B., 2017. Clinical and pathophysiological overview of acinetobacter infections: a century of challenges. Clin. Microbiol. Rev. 30, 409–447.
Wu, J.Y., Henins, K.A., Gressens, P., Gozes, I., Fridkin, M., Brenneman, D.E., Hill, J.M., 1997. Neurobehavioral development of neonatal mice following blockade of VIP during the early embryonic period. Peptides 18, 1131–1137.
Wymore Brand, M., Wannemuehler, M.J., Phillips, G.J., Proctor, A., Overstreet, A.M., Jergens, A.E., Orcutt, R.P., Fox, J.G., 2015. The altered schaedler flora: continued applications of a defined murine microbial community. ILAR J. 56, 169–178.